Rheol Acta (2015) 54:715–724
DOI 10.1007/s00397-015-0865-8

ORIGINAL CONTRIBUTION

Large amplitude oscillatory shear (LAOS) in model colloidal suspensions and glasses: frequency dependence

Andreas S. Poulos[1] · **Frédéric Renou**[2] · **Alan R. Jacob**[3] · **Nick Koumakis**[4] · **George Petekidis**[3]

Received: 7 May 2015 / Accepted: 17 June 2015 / Published online: 7 July 2015

Abstract We investigate the effect of frequency on the non-linear large amplitude oscillatory shear (LAOS) response of concentrated colloidal suspensions of model soft and hard spheres at various concentrations, both below and above the glass transition. We show that the anharmonic response in the stress increases with frequency for liquid-like samples but decreases with frequency for solid-like samples. We argue that for samples below the glass transition, higher frequencies involving higher maximum shear rates promote shear thinning and increase anharmonicity. On the other hand, solid-like samples deform plastically at low frequencies as they are subjected to low shear rates within the period. Higher frequencies (higher average shear rates) lead to viscous flow over a larger fraction of the period thereby decreasing anharmonic behavior. We also demonstrate that LAOS experiments in strain-controlled rheometry at moderately high frequencies (ω>5 rad/s) have to be very carefully interpreted, due to the superharmonic instrumental resonance effects.

Keywords Rheology · Colloids · Large amplitude oscillatory shear · Yielding · Glass transition

✉ Andreas S. Poulos
a.poulos@imperial.ac.uk

[1] Forschungszentrum Jülich, JCNS-1/ICS-1, 52428 Jülich, Germany

[2] URCOM, EA 3221, FR CNRS 3038, University of Le Havre, 25 rue Philippe Lebon, B.P. 1123, 76063 Le Havre, France

[3] IESL-FORTH and Department of Materials Science, University of Crete, Heraklion, Greece

[4] CNR-IPCF Dipartimento di Fisica, Università di Roma "La Sapienza", Rome, Italy

Introduction

Many common natural and industrial materials are composed of micrometer-sized solid particles dispersed in a liquid. Some examples of such colloidal dispersions are milk, blood, paint, and clays. From the above examples, it is clear that colloidal dispersions are relevant to a wide area of modern scientific research. In view of their many applications, an improved understanding of their flow behavior can be of immense practical significance (Mewis and Wagner 2011). It is well known that when the particulate volume fraction is increased, colloidal dispersions show pronounced non-Newtonian rheological behavior (Larson 1999; Mewis and Wagner 2011). At high-volume fraction, colloidal dispersions can also be trapped in metastable glassy states where individual particles cannot escape from cages formed by their neighbors (Pusey and van Megen 1987). These colloidal glasses present viscoelastic behavior and a yield stress, and their rheological response has been the subject of numerous publications (Mason and Weitz 1995; Senff and Richtering 1999; Fuchs and Cates 2002; Heymann et al. 2002; Petekidis et al. 2003; Besseling et al. 2007; Brader et al. 2010; van der Vaart et al. 2013).

A main feature of concentrated colloidal dispersions (similarly with other concentrated disordered soft materials) is that they show pronounced non-linear rheological behavior when subjected to large deformations (Mewis and Wagner 2011). The elucidation of non-linear response is essential for most applications and processes of biological or industrial significance, where large deformations and bidirectional flows are present. A commonly used method to study non-linear rheology is to extend linear small-amplitude oscillatory measurements to larger strain amplitudes. Thus, in a typical large amplitude oscillatory shear (LAOS) experiment, a sinusoidal strain of large amplitude is applied to the sample, and the non-sinusoidal stress response is measured (Philippoff 1966;

Dealy and Wissbrun 1990; Wilhelm et al. 1998; Cho et al. 2005; Helgeson et al. 2007; Ewoldt et al. 2008; Hyun et al. 2011). LAOS is different from the usual dynamic strain sweeps performed by most rheometers in that at each oscillatory strain amplitude, the full waveform of the stress response is recorded and analyzed and not just the first harmonic of the stress that gives G' and G".

Several methods of analyzing LAOS data have been proposed and recently reviewed in the literature (Wilhelm et al. 1998; Cho et al. 2005; Klein et al. 2007; Hyun et al. 2011; Rogers et al. 2011; Poulos et al. 2013). The most common method is Fourier transform (FT) analysis, where the non-sinusoidal but periodic stress response to LAOS is expressed as a Fourier series (Wilhelm et al. 1998; Wilhelm et al. 1999). The magnitude of non-linear, or anharmonic, response can thus be quantified very accurately by the relative amplitudes of higher odd harmonics with respect to the fundamental, while even harmonics are expected to be absent due to symmetry reasons unless phenomena like slip are present. This approach has been used extensively to analyze LAOS results on a variety of systems such as linear polymers (Wilhelm et al. 2000), branched polymers (Schlatter et al. 2005), cubic phases of diblock and triblock copolymer micelles (Daniel et al. 2001; Nicolai and Benyahia 2005; Hyun et al. 2006; López-Barrón et al. 2012), and concentrated colloidal suspensions (Heymann et al. 2002; Le Grand and Petekidis 2008; Carrier and Petekidis 2009; Brader et al. 2010; Lin et al. 2013).

LAOS has become one of the most common techniques to study non-linear response because one can change independently the oscillation amplitude γ_0 and the frequency ω, essentially probing the whole range of rheological behavior, from steady shear flow and linear viscoelasticity to non-linear viscoelasticity (Hyun and Wilhelm 2009; Hyun et al. 2011). However, although LAOS experiments have regularly been performed on colloidal suspensions, most often they are constrained to a single oscillatory frequency. Only recently, hard sphere glasses have been investigated by experimental rheometry and Brownian dynamics (BD) simulations in a wider frequency range bridging the low-frequency Brownian-dominated regime with the high-frequency regime where shear-induced non-Brownian dynamics are prominent (Koumakis et al. 2013). Moreover, confocal microscopy experiments of a sheared hard-sphere colloidal suspension provided new insight into the structural changes as a function of frequency under large amplitude oscillatory shear but without measuring the rheological properties at the same time (Lin et al. 2013).

Here, we present LAOS measurements at multiple frequencies on model concentrated colloidal dispersions of star-like micelles and sterically stabilized poly-methylmethacrylate (PMMA) hard spheres, below and above the glass transition volume fraction. Both systems are already very well characterized and represent the two extremes in interparticle potential (ultrasoft versus almost hard sphere-like). Ultrasoft star-like micelles (Renou et al. 2010a; Koumakis et al. 2012; Poulos et al. 2013), similar multi-arm star polymers (Helgeson et al. 2007; Rogers et al. 2011), and soft core-shell microgels (Carrier and Petekidis 2009; Brader et al. 2010) have been studied experimentally by LAOS before but mainly at low frequencies.

We show that frequency variation even over a relatively small range of one order of magnitude can profoundly affect the LAOS response. Moreover, we conclusively show that an increase in frequency has opposing effects depending on whether the colloidal dispersion is in a liquid or glassy state; it leads to increasing anharmonic behavior below the glass transition but decreasing anharmonic response above the glass transition. We explain the observed variation of non-linearity with frequency above and below the glass transition using recent insights that relate the LAOS response with the linear (SAOS) response and the flow curve of the material. Moreover, in the Appendix, we demonstrate the difficulty of performing even moderately high-frequency LAOS measurements (ω>5 rad/s) by showing evidence of a previously unreported rheometer transducer resonance effect in strain-controlled instruments that introduces strong higher harmonics, precluding the detection of the true sample response.

Materials and methods

Star-like micelles from PEP–PEO block copolymers

Poly(ethylene-alt-propylene)–poly(ethylene oxide) block copolymers were prepared by a two-step anionic polymerization (Allgaier et al. 1997). The number-average molar mass (M_n) was 1300 g/mol for the PEP block and 20,300 g/mol for the PEO block corresponding to an overall M_n=21,600 g/mol for the block copolymer. Poly(ethylene-alt-propylene)–poly(ethylene oxide) (PEP–PEO) block copolymers with this block ratio form micelles in deuterium oxide (D_2O) with an aggregation number of 120 and a pair interaction potential similar to regular star polymers (Laurati et al. 2005). Previous work has demonstrated that no kinetic exchange of arms between micelles is possible (Stellbrink et al. 2004; Lund et al. 2006). The absence of kinetic exchange ensures that the aggregation number remains constant with varying concentration and temperature. The micelles can thus be considered as stable colloidal entities with star-like pair interactions. Clear solutions were obtained by dissolving the PEP–PEO polymer in deuterium oxide (D_2O 99.8 % atom D purchased by Armar Chemicals). The solutions were left to equilibrate at room temperature for at least 1 week before measurement. The effective volume fraction ϕ_{eff} estimated as the ratio of the concentration, c, to the overlap concentration, c* (=3 $M/4\pi N_A R_h^3$), is calculated by using the polymer concentration and measured by dynamic light scattering hydrodynamic radius of the micelles R_h=

36 nm (in dilute solutions). As the micelles can interpenetrate, ϕ_{eff} may take values above one.

Poly-methylmethacrylate hard sphere colloids

Furthermore, for comparison, a model hard-sphere (HS) colloidal suspension was used for some of the experiments (Pusey and van Megen 1987). The HS particles consist of a poly-methylmethacrylate (PMMA) core and a sterically stabilizing chemically grafted poly-hydrostearic acid (PHSA) layer (10 nm) (Koumakis et al. 2012). The mean radius of the HS spheres used here is either R=106 nm or R=196 nm, with a polydispersity of about 10 % to prevent effects from shear-induced crystallization (Koumakis et al. 2008). Dispersion in an octadecene/bromonaphthalene mixture (with a refractive index of 1.485) was used to eliminate evaporation during the rheological measurements.

Experimental methods

An Anton-Paar Physica MCR 501 stress-controlled rheometer was used in strain-control mode for the LAOS experiments at low frequencies, using the direct strain oscillation (DSO) mode. We used a stainless steel cone-and-plate geometry, with a cone diameter of 50 mm, an angle of 0.04 rad, and a truncation (gap) of 50 μm. High-frequency LAOS measurements were performed using a strain-controlled rheometer ARES (Rheometrics Scientific/TA) with a force rebalance transducer 100FRTN1 in cone-plate geometry (25 mm diameter with a cone angle of 0.048 rad and 50 mm diameter with an angle of 0.01 rad). For both rheometers, the temperature was controlled by a Peltier system, and a home-made solvent trap was used to minimize evaporation during measurements typically lasting up to at least 4 h. The use of different types of stress and strain-controlled rheometers for LAOS measurements as well as different measuring geometries has been recently discussed for some of the rheometers used here (Merger and Wilhelm 2014; Giacomin et al. 2015).

Results and discussion

PEP–PEO star-like micelles with 120 arms exhibit a liquid-to-glass transition at an effective volume fraction of ϕ_{eff}=2.5 (Renou et al. 2010a; Koumakis et al. 2012), significantly higher than hard spheres (ϕ≈0.59) and in line with regular multi-arm star polymers of similar functionality (Stiakakis et al. 2002; Helgeson et al. 2007; Erwin et al. 2010; Stiakakis et al. 2010). The transition was determined from linear viscoelastic measurements that show a progressive increase of the elastic modulus G', as well as the appearance of an apparent yield stress in steady shear flow (Koumakis et al. 2012). Here, we compare the LAOS response of solutions at low (liquid-like) and high (solid-like) concentrations. The linear dynamic frequency sweeps of two representative samples can be seen in Figs. 1a and 2a, respectively. The low concentration solution (ϕ_{eff}=2.3) presents a typical viscoelastic liquid response with a crossover frequency of 16 rad/s. In the 0.5–5 rad/s frequency range where we perform LAOS experiments, the material response has a predominant viscous character. On the other hand, the high-concentration solution (ϕ_{eff}=3.1) has all the characteristics of a soft glass. It

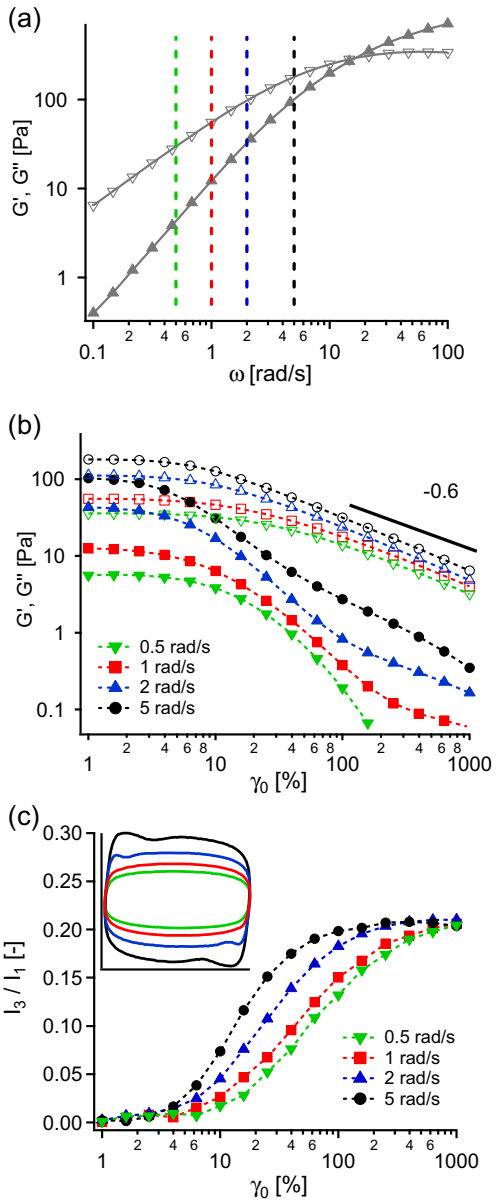

Fig. 1 **a** Dynamic frequency sweep (G' (*filled triangles*), G" (*open triangles*)) of star-like micelles at an effective volume fraction ϕ_{eff}=2.3, below the glass transition. **b** Dynamic strain sweeps of the same sample at different frequencies. G', G" are shown with *filled* and *open symbols*, respectively: ω=0.5 rad/s (*inverted green triangles*), ω=1 rad/s (*red squares*), ω=2 rad/s (*blue triangles*), and ω=5 rad/s (*black circles*). **c** Normalized amplitudes of the third harmonic. Inset: Lissajous figures (stress vs strain) of the full waveforms for the selected frequencies at a non-linear amplitude γ_0=100 %

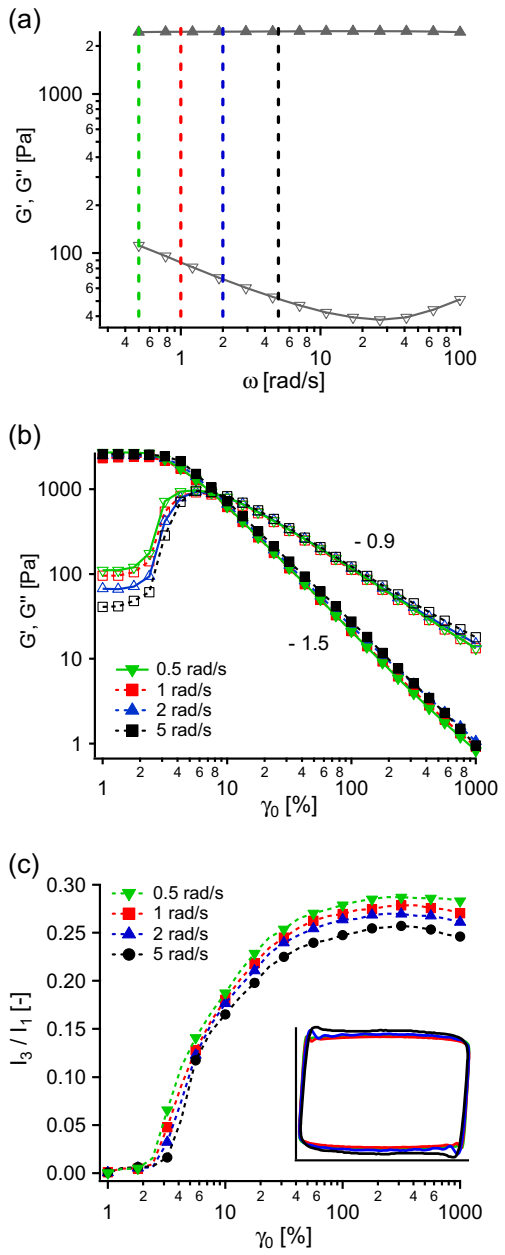

Fig. 2 **a** Dynamic frequency sweep (G' (*filled triangles*), G" (*open triangles*)) of star-like micelles at high effective volume fraction ϕ_{eff}= 3.1, above the glass transition. **b** Dynamic strain sweeps of the same sample at different frequencies. G', G" are shown with *filled* and *open symbols*, respectively: ω=0.5 rad/s (*inverted green triangles*), ω=1 rad/s (*red squares*), ω=2 rad/s (*blue triangles*), and ω=5 rad/s (*black circles*). **c** Normalized amplitudes of the third harmonic. Inset: Lissajous figures (stress vs strain) of the full waveforms for the selected frequencies at a non-linear amplitude γ_0=100 %

presents a frequency independent elastic response, with G' greater than G" by more than one order of magnitude, while the increase of G" at low ω indicates the existence of a slower relaxation process outside of our experimental window (Mason and Weitz 1995). The linear frequency sweeps unambiguously demarcate the liquid-to-solid transition.

Non-linear LAOS experiments were performed at different frequencies on six samples, three below the glass transition (ϕ_{eff}=2.15, 2.3, 2.35) and three above the glass transition (ϕ_{eff}=2.8, 2.9, 3.1) using the Anton-Paar (MCR-501) rheometer. For each frequency, the strain amplitude γ_0 was varied from 1 %, where the stress response is linear, to 1000 %. The dynamic strain sweeps obtained for the two representative samples can be seen in Figs. 1b and 2b, respectively. For the liquid-like sample, the linear regime is directly followed by a power law decrease of G" with γ_0, with an exponent of −0.6. On the other hand, for the solid-like sample, G" presents a peak just beyond the linear regime, which is a typical feature of yielding in colloidal glasses (Mason and Weitz 1995; Mason et al. 1996; Pham et al. 2006; Helgeson et al. 2007). At large γ_0, both G' and G" decrease as power laws with exponents −1.5 and −0.9, respectively, as discussed before (Koumakis et al. 2012). The stress signal was further analyzed at each strain amplitude by FT rheology, and the non-linearity was quantified by the amplitude of the 3rd stress harmonic normalized by the 1st harmonic (I_3/I_1) (Wilhelm et al. 1998). It should be noted that in general, higher harmonics are also important (Poulos et al. 2013) and that there are other analysis methods used to quantify non-linearity (Hyun et al. 2011), but for the purposes of this study, we follow I_3/I_1 as an indicator of the level of anharmonic stress response in the non-linear oscillatory shear.

The LAOS amplitude and frequency dependence of the representative liquid-like sample is shown in Fig. 1c. The chosen frequency range means that all LAOS experiments are performed at frequencies where G" > G' in the linear regime. As expected, the non-linearity at all frequencies increases with strain amplitude up to about I_3/I_1=20 % reached at γ_0=1000 %. More importantly, we see that as the frequency is increased, the onset of non-linearity takes place at lower γ_0 and remains higher over the whole range of strain amplitudes investigated here. However, the maximum 3rd harmonic contribution attained is essentially independent of ω. In Fig. 2c, the same graph is plotted for the representative solid-like sample, where G' > G" in the linear regime. Here, the curves at different frequencies appear very similar; a clear difference appears only at γ_0>20 %. Compared to the liquid-like sample, I_3/I_1 increases much more sharply with γ_0. Moreover, the third harmonic non-linearity reaches higher values of between 23 and 28 %, depending on the frequency. In summary, for the ultrasoft star-like micelles, the anharmonicity for liquid-like samples mainly depends on the frequency of oscillation while for the solid-like sample, differences between each frequency are only visible when the strain amplitude is quite high. This observation reveals that the LAOS response of a system is related to its linear response.

In Fig. 3, we compare the frequency dependence of I_3/I_1 at γ_0=100 % for the six star-like micelle samples. It becomes clear that for the liquid-like samples, the non-linear,

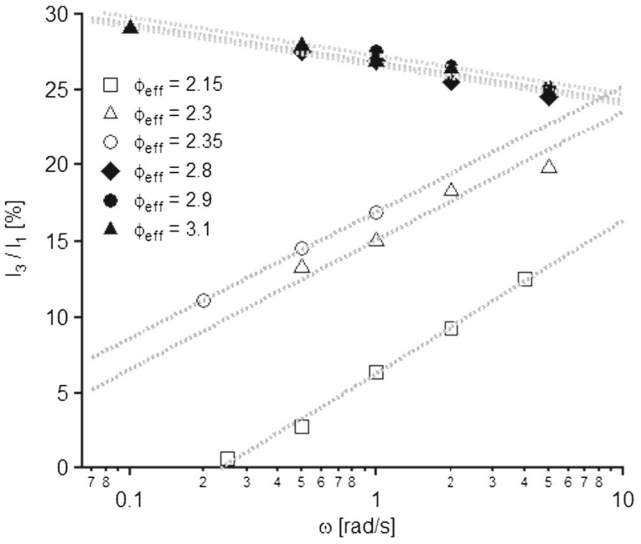

Fig. 3 Normalized third harmonic (I_3/I_1) as a function of LAOS frequency for three solid-like ϕ_{eff}=2.8 (*diamonds*), 2.9 (*filled circles*), and 3.1 (*filled trinagles*) and three liquid-like ϕ_{eff}=2.15 (*open squares*), 2.3 (*open triangles*), and 2.35 (*open circles*) samples, measured at a non-linear strain amplitude of 100 %. It can be seen that the non-linearity increases with frequency for the liquid-like samples but decreases with frequency for the solid-like samples

anharmonic behavior becomes more important as ω is increased while the opposite is observed for the solid-like samples. Thus, the nature of the state at rest of the colloidal dispersion affects directly the frequency dependence of the non-linearity under LAOS. An increase of LAOS frequency has the opposite effect depending on whether the material is at a liquid-like or a glassy state.

The variation of I_3/I_1 with frequency can be phenomenologically described by the simple equation, $^{I_3}/_{I_1} = A\ln(\omega/\omega_c)$, where A and ω_c are constants that depend on the volume fraction. This equation has been used to generate the fits shown in Fig. 3. The constant A is positive for samples below the glass transition and negative for samples above the glass transition.

To rationalize such different response of the anharmonicity, as represented by I_3/I_1, below and above the glass transition, we point out that while for colloidal liquids a finite structural relaxation time (τ_{rel}) which is commonly estimated as the inverse of the crossover angular frequency in the dynamic frequency sweep exists, colloidal glasses have very long, if not infinite, relaxation times. Thus, for the ϕ_{eff}=2.3 sample, the relaxation time is τ_{rel}~0.06 s, whereas for the sample with ϕ_{eff}=3.1, this is over 100 s (Renou et al. 2010a). The latter also exhibits a yield stress below which the material will not flow, at least in a time scale shorter than the experimental one. Moreover, the stresses introduced under shear (and the underlying structure) may not relax quickly and fully, even when shear is stopped (Ballauff et al. 2013). This difference is made evident in Fig. 4 where the flow curves of the two materials are shown. Below a shear rate of 0.1 s^{-1}, the colloidal liquid flows with a constant viscosity whereas the colloidal glass shows a yield stress plateau (~40 Pa), where a continuous deformation would lead to plastic flow.

Non-linear viscoelasticity under LAOS can be partly understood, at least qualitatively, by referring to the equilibrium rheological properties of the material measured by a dynamic frequency sweep (Figs. 1a and 2a) and the flow curve measured by a steady rate sweep (Fig. 4) (Poulos et al. 2013). These represent the two limiting behaviors $\gamma_0 \rightarrow 0$ and $\omega \rightarrow 0$, respectively. By definition, a dynamic frequency sweep is the low amplitude limit of LAOS. Moreover, it is reasonable to assume that LAOS at the limit of zero frequency can be reproduced by the flow curve alone (Sollich 1998), although in practice, this is not possible at the usual LAOS frequencies for most systems where the relaxation time is finite (i.e., non zero) since within a period of oscillation, the shear rate is constantly changing faster than the system relaxes (Poulos et al. 2013). Hence, for a purely viscous system, the structure has enough time to relax at all points inside the period since its relaxation time is much shorter than the inverse of the shear rate.

For finite LAOS frequencies, whether or not, we attain the $\omega \rightarrow 0$ limit depending on how rapidly the system relaxes. The liquid-like sample is probed at frequencies below the (linear) crossover frequency. This suggests that the structure has time to fully relax during LAOS, and memory (elastic) effects are not significant. Hence, the stress non-linearity is dictated by shear thinning alone. As the frequency is increased, higher shear rates are reached leading to stronger shear thinning and higher I_3/I_1. This can also be seen from the liquid-like flow curve in Fig. 4 where the maximum shear rate reached for each LAOS frequency is indicated with a vertical line. It is clear that for the frequencies used here, the maximum rate corresponds to the shear-thinning regime of the flow curve.

For solid-like samples, when γ_0 approaches the yield strain of the material, the stress waveform becomes distorted as there are alternatively regions of elastic response (before yielding)

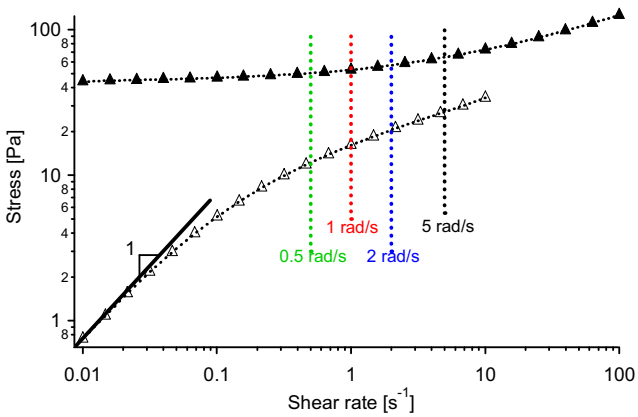

Fig. 4 Steady state flow curves (stress versus rate) for a liquid-like ϕ_{eff}= 2.3 (*open triangles*) and a solid-like ϕ_{eff}=3.1 (*filled triangles*) solution of star-like micelles. The *vertical lines* denote the maximum shear rate in a LAOS experiment with γ_0=100 % and frequency indicated in the figure

and plastic/viscous response (after yielding) within a LAOS cycle (Renou et al. 2010a; Rogers et al. 2011). At strain amplitudes much greater than the yield strain (γ_0~100 %), the Lissajous plot becomes box-like because even after yielding, the material deforms plastically as the relevant shear rates are at the yield stress plateau (Fig. 4). However, as the frequency is increased further, strain rates beyond the yield stress plateau are reached. During a fraction of the period, around maximum shear rate, the material starts flowing more like a Newtonian liquid (approaching a rate-independent viscosity). This will tend to decrease the anharmonic stress response compared to the case of only plastic deformation. Hence, for solid-like material, the anharmonicity decreases with frequency as higher strain rates beyond the yield stress plateau are reached and the material flows during a larger fraction of the period.

Therefore, the difference in the frequency dependence of I_3/I_1 between the liquid-like and the solid-like sample originates from the increasing shear rates at higher frequencies. For the liquid-like sample, increasing rate means moving towards the shear-thinning region of the flow curve while for the solid-like sample, increasing rate leads from plastic flow to viscous flow. In the first case, the viscosity changes over the period of oscillation introducing higher harmonics while in the second case, the stress starts to follow the shear rate, reducing

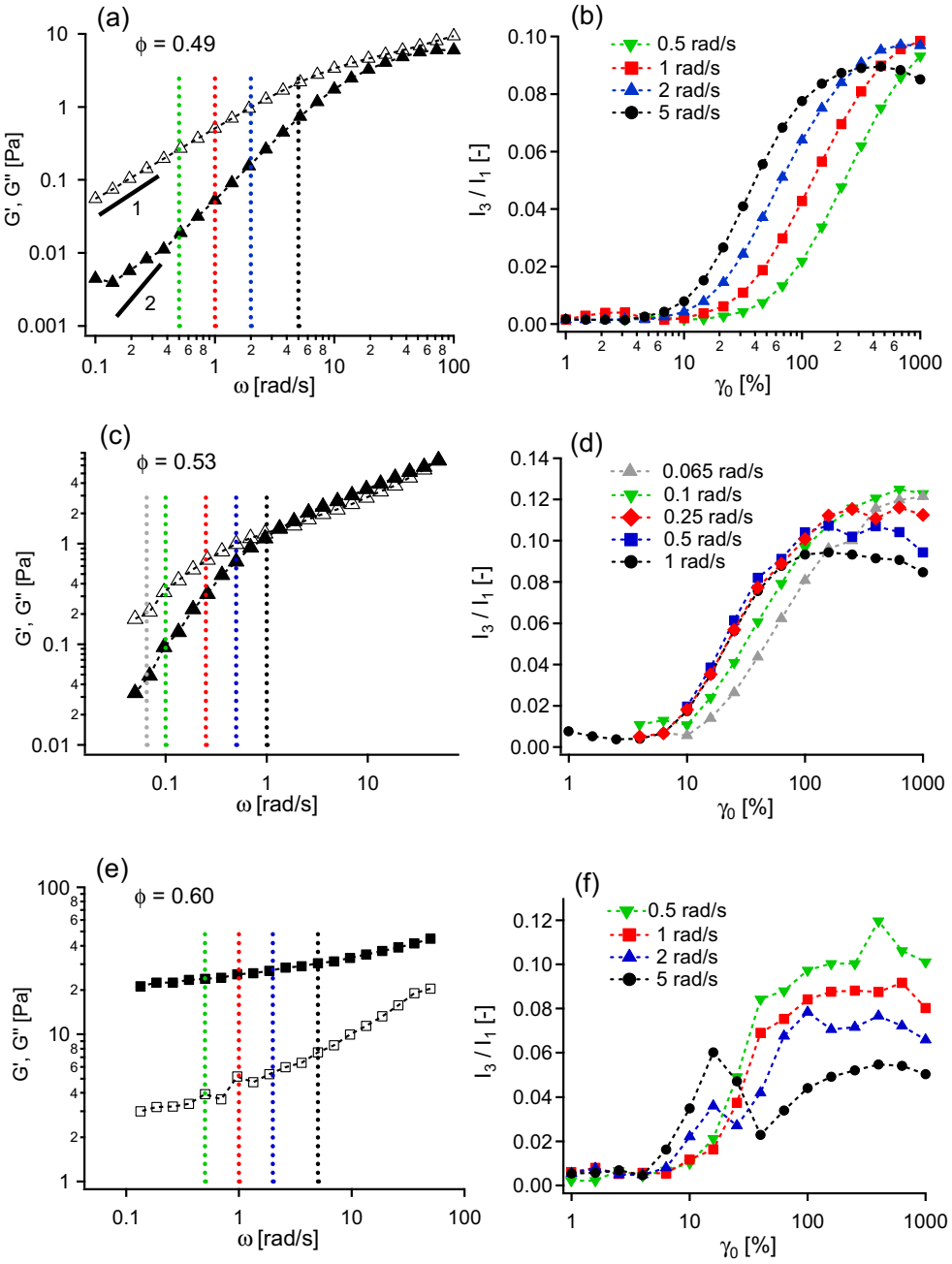

Fig. 5 Dynamic frequency sweeps (*left column*: G' (*filled triangles*), G" (*open triangles*)) and normalized third harmonic I_3/I_1 (*right column*) of PMMA hard-sphere particles. The volume fractions are respectively for (**a**) and (**b**) ϕ=0.49, for (**c**) and (**d**) ϕ=0.53, and for (**e**) and (**f**) ϕ=0.6

anharmonicity during a transition from a plastic to a liquid-like flow. In this sense, the non-linearities should decrease at regimes where simple Newtonian flow is approached.

Frequency variation in hard spheres

In order to validate a universal behavior in different colloidal systems, we conducted a similar study for PMMA hard spheres. In this case, we compare the LAOS frequency dependence of four HS samples at ϕ=0.49, 0.53, 0.54, and 0.60. The dynamic frequency sweeps of the ϕ=0.49, 0.53, and 0.60 samples can be seen in Fig. 5a, c, and e, respectively. It is clear that the high-concentration sample is in the glassy state; the intermediate concentration is liquid and shows a crossover of G' and G", and the low concentration sample shows terminal liquid-like behavior (G' $\propto \omega^2$, G" $\propto \omega$) in a wide frequency range.

Dynamic strain sweeps are again performed at different frequencies on all samples. In Fig. 5b, d, and f, I_3/I_1 is plotted as a function of γ_0 for the ϕ=0.49, 0.53, and 0.60 samples, respectively. It can be seen that the variation is similar to star-like micelles, with I_3/I_1 increasing at yielding and developing to a plateau at high γ_0. One major difference is that for the highest concentration glassy sample (ϕ=0.60), a peak in I_3/I_1 appears at intermediate amplitudes (γ_0~10–30 %) for the two highest frequencies (Fig. 5f); this has been attributed before to a second yielding process and will be discussed below (Koumakis et al. 2013).

In Fig. 6, I_3/I_1 is plotted as a function of ω at a fixed amplitude of 100 % strain, for all volume fractions. Similar to star-like micelles (Fig. 3), the highest concentration glassy sample (ϕ=0.60) shows a decrease of I_3/I_1 with frequency, and the lowest concentration liquid sample (ϕ=0.49) shows an increase of I_3/I_1 in the frequency regime measured.

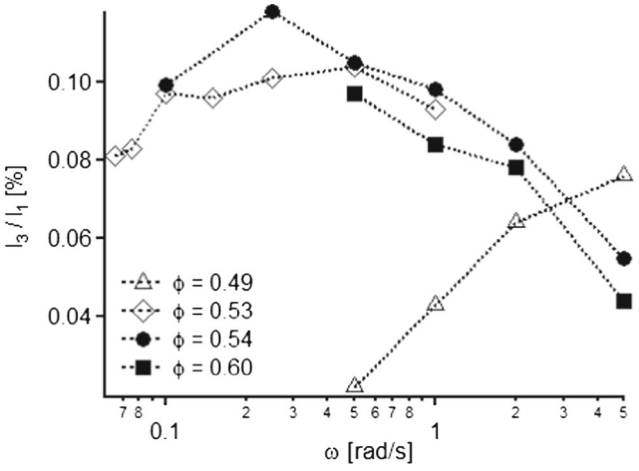

Fig. 6 Normalized third harmonic (I_3/I_1) as a function of LAOS frequency for four HS samples with ϕ=0.49 (*open triangles*), 0.53 (*open diamonds*), 0.54 (*filled circles*), and 0.6 (*filled squares*), measured at a non-linear strain amplitude of 100 %

Additionally, the intermediate ϕ=0.53 and 0.54 samples show non-monotonic behavior with I_3/I_1 increasing at low frequencies and decreasing at high frequencies.

For HS glasses, a decrease of I_3/I_1 with increasing frequency has been seen before (Koumakis et al. 2013). Combining experiments and Brownian dynamics simulations, it was attributed to the transition from a plastic-like response to a simpler liquid-like response while also finding a different yielding process emerging at even higher frequencies. Lower frequencies were associated with Brownian activated yielding, while higher frequencies to shear-induced non-Brownian yielding. The peak of I_3/I_1 found for increasing strain at higher frequencies was attributed to the appearance of this second yielding process. For intermediate HS volume fractions, the frequency dependence of I_3/I_1 shows a broad peak (Fig. 6). In contrast to the case of star-like micelles, where the chosen frequencies were taken far from the crossover of G' and G", the hard-sphere data shows the transitional behavior expected near that point. Therefore, it shows an increasing I_3/I_1 versus ω, where the linear response is liquid-like and decreasing I_3/I_1 when the linear response becomes solid-like.

The similarities in the behavior of I_3/I_1 between hard spheres and star-like micelles suggest an independence from specific particle interactions. In the case of hard spheres, I_3/I_1 versus ω eventually reached a minimum and then started to increase again at higher ω. We may expect similar effects for the star-like micelles; however, to observe this non-monotonic variation of I_3/I_1, we need to go to frequencies much higher than 5 rad/s.

Conclusions

In this paper, we investigated the effect of frequency on the non-linear oscillatory (LAOS) response of two model colloidal dispersions: soft star-like micelles and PMMA hard spheres. LAOS experiments were performed at a range of frequencies on six colloidal star-like micelle samples above and below the glass transition. We showed that an increase in frequency from 0.5 to 5 rad/s leads to an increase of anharmonicity for the liquid-like samples, but to a decrease of anharmonicity for the solid-like samples. We argue that the difference can be explained by looking at the contribution to non-linearity at the maximum shear rate inside the period of oscillation. As the frequency is increased, the maximum shear rate is also increased. Thus, for the liquid-like samples, higher shear rates lead to shear thinning over a larger fraction of the period thereby increasing anharmonicity. On the other hand, the solid-like samples at low shear rates are trapped in the yield stress plateau and do not flow but deform plastically. Higher shear rates lead to viscous flow over a larger fraction of the period thereby decreasing anharmonicity.

These findings are corroborated by the hard sphere system, suggesting an independence from details of the interparticle interactions. Similar to star-like micelles, the liquid-like suspensions show increasing anharmonicity with frequency. For the solid-like suspensions, a decrease of I_3/I_1 frequency is again attributed to the transition from a plastic-like response to a simpler liquid-like response. On the other hand, the transition and change in slope of I_3/I_1 from solid- to liquid-like samples are broader at the intermediate volume fraction HS samples where the storage and loss moduli have not reached the terminal regime.

Acknowledgments We acknowledge J. Stellbrink and L. Willner for providing the PEP1–PEO20 diblock copolymer and A.B.. Schofield for providing the PMMA particles. We also thank J. Stellbrink for the helpful discussions and comments on the manuscript. We also acknowledge the financial support by the DFG within SFB TR6 (project A2) and the Greek project Thales "Covisco".

Appendix

Oscillatory rheometry at high frequencies

We have measured the LAOS response of all samples at a relatively limited range of frequencies (0.1–5 rad/s). Measuring at higher frequencies is essential to enter the domain of non-linear viscoelasticity and gain a more complete understanding of the processes involved. For these samples, the stress-controlled Anton-Paar MCR 501 rheometer does not produce perfect sinusoidal large-amplitude deformations through the direct strain control (DSO) feedback loop, introducing additional artificial higher harmonics in the stress signal. Hence, in order to perform high-frequency (ω>5 rad/s) LAOS measurements, a strain-controlled ARES rheometer with a 100FRTN1 force rebalance transducer was also used. However, as we will show below, the interpretation of non-linear data was not possible due to the transducer resonance effect that introduced higher harmonics even at moderate frequencies, above about 10 rad/s.

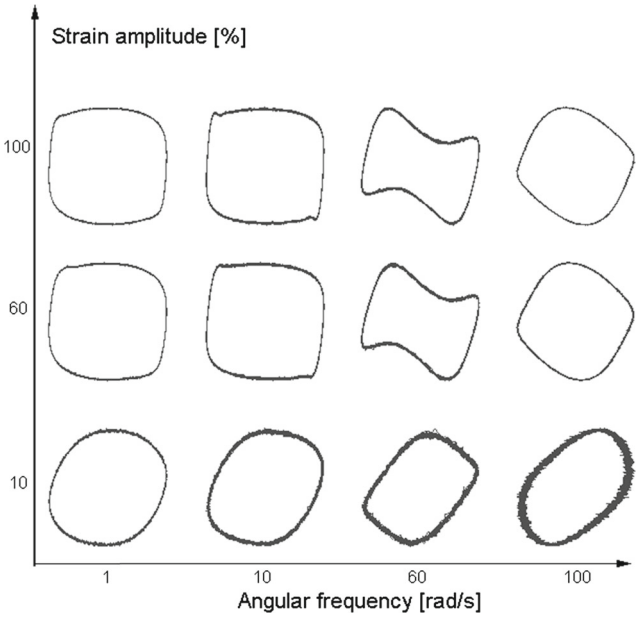

Fig. 8 Pipkin plot showing Lissajous figures (stress vs strain) for selected data. The star-like micelle sample is at ϕ_{eff}=3.1. Note the unconventional shapes at ω=60 rad/s

Dynamic time sweeps were performed at different amplitudes and frequencies on the solid-like star-like micelle samples. The normalized third and fifth harmonics, I_3/I_1 and I_5/I_1, are plotted in a Pipkin-type diagram (I_n/I_1 vs amplitude γ_0 and frequency ω). The resulting contour plots are shown in Fig. 7. Both I_3/I_1 and I_5/I_1 show a well-defined peak in the Pipkin space. The third harmonic peak is at γ_0=100 % and ω=65 rad/s and the fifth harmonic peak at the same amplitude γ_0= 100 %, but lower frequency ω=40 rad/s. Furthermore, at the peak, the non-linearity is extremely large; it reaches values of 48 % for the third harmonic and 24 % for the fifth which are quite unusual. In comparison, the non-linearity in the low-frequency regime saturates at I_3/I_1=28 % (Fig. 2c). The Lissajous figures for selected data points can be seen in Fig. 8 in a Pipkin representation. It is clear that the shape drastically changes at around ω=60 rad/s. The maximum stress that follows strain reversal is dominating the response,

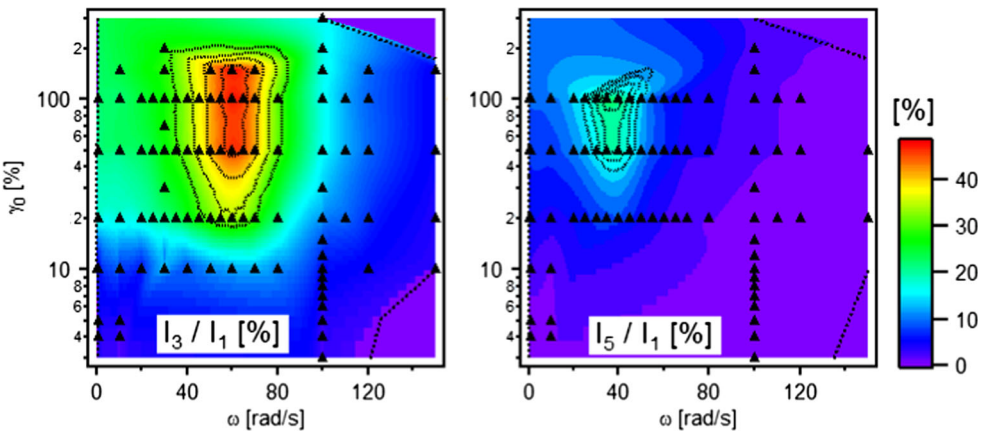

Fig. 7 Normalized amplitude of the third and fifth Fourier harmonics of the stress response of star-like micelles at ϕ_{eff}=3.1. A peak in I_n/I_1 can be observed at an angular frequency of 60 rad/s in the case of the third harmonic and at 40 rad/s in the case of the fifth harmonic

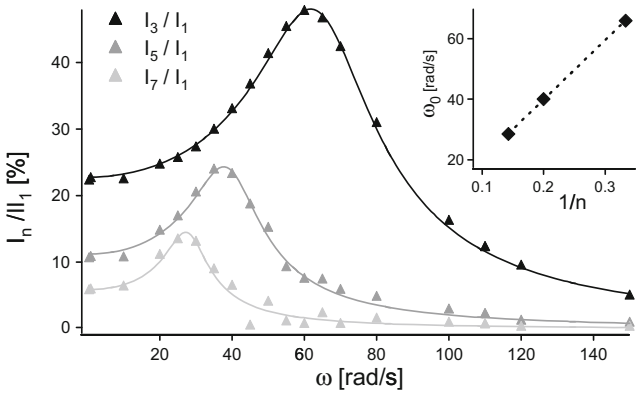

Fig. 9 Fit of the normalized amplitude of higher harmonics. *Lines* represent fit using the damped, driven harmonic oscillator equation. Inset: resonance frequency ω_0 vs $1/n$, where n is the harmonic number

and it is followed by a stress minimum close to maximum shear rate.

In Fig. 9, we show the variation of the third, fifth, and seventh harmonic with frequency at an amplitude γ_0= 100 %. All three normalized harmonics can be fitted with a damped, driven harmonic oscillator equation:

$$\frac{I_n}{I_1} = \frac{\alpha}{\sqrt{\left(\omega^2 - \omega_0^2\right)^2 + \beta^2\omega^2}}$$

where ω_0 is the resonance frequency, β is the damping parameter, and α is the normalized amplitude. The lines in Fig. 9 indicate least-squares fitting of the data with the resonance equation, which gives excellent agreement and a resonance frequency of 66, 40, and 28 rad/s for the third, fifth, and seventh harmonics, respectively. In the inset of Fig. 9, we show that the resonance frequencies are proportional to $1/n$ (where n is the number of the harmonic). This is typical of non-linear or superharmonic resonance effect which corresponds to resonance of the higher harmonics at integer fractions of the natural (or fundamental) frequency of a driven non-linear oscillator. Extrapolation of the line (inset, Fig. 9) to where $1/n$ is equal to one gives a fundamental resonance frequency of 200 rad/s.

In order to verify this resonance effect, we also used PMMA hard spheres at ϕ=0.6. A similar resonance peak is visible at a lower amplitude of 20 % but crucially at the same frequency of 65 rad/s. The fact that resonance appears at the same frequencies for samples as different as star-like micelles and PMMA hard spheres, as well as the unnaturally high values of non-linearity, points out to an instrumental origin of the non-linear resonance effect.

It is important to realize that the transducer of the rheometer has a feedback loop that keeps the measurement geometry in place, and the torque measured is just proportional to the reaction torque that drives the tool back to the original position. This feedback loop has a characteristic time constant in the tens of milliseconds range (Dullaert and Mewis 2005) and can thus be driven to resonance at frequencies around hundreds of rad/s. Thus, a fundamental frequency of 200 rad/s is consistent with the view that the superharmonic resonance effect is caused by the transducer and not by the sample.

References

Allgaier J, Poppe A, Willner L, Richter D (1997) Synthesis and characterization of poly 1,4-isoprene-b-(ethylene oxide) and poly ethylene-co-propylene-b-(ethylene oxide) block copolymers. Macromolecules 30:1582–1586. doi:10.1021/ma961311q

Ballauff M, Brader JM, Egelhaaf SU, Fuchs M, Horbach J, Koumakis N, Krüger M, Laurati M, Mutch KJ, Petekidis G, Siebenbürger M, Voigtmann T, Zausch J (2013) Residual stresses in glasses. Physical Review Letters 110. doi:10.1103/PhysRevLett.110.215701

Besseling R, Weeks ER, Schofield AB, Poon WCK (2007) Three-dimensional imaging of colloidal glasses under steady shear. Phys Rev Lett 99:028301. doi:10.1103/PhysRevLett.99.028301

Brader JM, Siebenbürger M, Ballauff M, Reinheimer K, Wilhelm M, Frey SJ, Weysser F, Fuchs M (2010) Nonlinear response of dense colloidal suspensions under oscillatory shear: Mode-coupling theory and Fourier transform rheology experiments. Phys Rev E 82. doi:10.1103/PhysRevE.82.061401

Carrier V, Petekidis G (2009) Nonlinear rheology of colloidal glasses of soft thermosensitive microgel particles. J Rheol 53:245–273. doi:10.1122/1.3045803

Cho KS, Hyun K, Ahn KH, Lee SJ (2005) A geometrical interpretation of large amplitude oscillatory shear response. J Rheol 49:747. doi:10.1122/1.1895801

Daniel C, Hamley IW, Wilhelm M, Mingvanish W (2001) Non-linear rheology of a face-centred cubic phase in a diblock copolymer gel. Rheol Acta 40:39–48. doi:10.1007/s003970000124

Dealy JM, Wissbrun KF (1990) Melt rheology and its role in plastics processing. Springer

Dullaert K, Mewis J (2005) Stress jumps on weakly flocculated dispersions: steady state and transient results. J Colloid Interface Sci 287: 542–551

Erwin BM, Cloitre M, Gauthier M, Vlassopoulos D (2010) Dynamics and rheology of colloidal star polymers. Soft Matter 6:2825. doi:10.1039/b926526k

Ewoldt RH, Hosoi AE, McKinley GH (2008) New measures for characterizing nonlinear viscoelasticity in large amplitude oscillatory shear. J Rheol 52:1427. doi:10.1122/1.2970095

Fuchs M, Cates ME (2002) Theory of nonlinear rheology and yielding of dense colloidal suspensions. Phys Rev Lett 89:248304. doi:10.1103/PhysRevLett.89.248304

Giacomin AJ, Gilbert PH, Merger D, Wilhelm M (2015) Large-amplitude oscillatory shear: comparing parallel-disk with cone-plate flow. Rheol Acta 54:263–285. doi:10.1007/s00397-014-0819-6

Helgeson ME, Wagner NJ, Vlassopoulos D (2007) Viscoelasticity and shear melting of colloidal star polymer glasses. J Rheol 51:297–316. doi:10.1122/1.2433935

Heymann L, Peukert S, Aksel N (2002) Investigation of the solid–liquid transition of highly concentrated suspensions in oscillatory amplitude sweeps. J Rheol 46:93. doi:10.1122/1.1423314

Hyun K, Nam JG, Wilhelm M, Ahn KH, Lee SJ (2006) Large amplitude oscillatory shear behavior of PEO-PPO-PEO triblock copolymer solutions. Rheol Acta 45:239–249. doi:10.1007/s00397-005-0014-x

Hyun K, Wilhelm M (2009) Establishing a new mechanical nonlinear coefficient Q from FT-rheology: first investigation of entangled

linear and comb polymer model systems. Macromolecules 42:411–422. doi:10.1021/ma8017266

Hyun K, Wilhelm M, Klein CO, Cho KS, Nam JG, Ahn KH, Lee SJ, Ewoldt RH, McKinley GH (2011) A review of nonlinear oscillatory shear tests: analysis and application of large amplitude oscillatory shear (LAOS). Prog Polym Sci 36:1697–1753. doi:10.1016/j.progpolymsci.2011.02.002

Klein CO, Spiess HW, Calin A, Balan C, Wilhelm M (2007) Separation of the nonlinear oscillatory response into a superposition of linear, strain hardening, strain softening, and wall slip response. Macromolecules 40:4250–4259. doi:10.1021/ma062441u

Koumakis N, Brady JF, Petekidis G (2013) Complex oscillatory yielding of model hard-sphere glasses. Physical Review Letters 110(5): 178301. doi:10.1103/PhysRevLett.110.178301

Koumakis N, Pamvouxoglou A, Poulos A, Petekidis G (2012) Direct comparison of the rheology of model hard and soft particle glasses. Soft Matter 8:4271–4284

Koumakis N, Schofield AB, Petekidis G (2008) Effects of shear induced crystallization on the rheology and ageing of hard sphere glasses. Soft Matter 4:2008. doi:10.1039/b805171b

Larson R (1999) The structure and rheology of complex fluids. Oxford University Press, New York

Laurati M, Stellbrink J, Lund R, Willner L, Richter D, Zaccarelli E (2005) Starlike micelles with starlike interactions: a quantitative evaluation of structure factors and phase diagram. Physical Review Letters 94. doi:10.1103/PhysRevLett.94.195504

Le Grand A, Petekidis G (2008) Effects of particle softness on the rheology and yielding of colloidal glasses. Rheol Acta 47:579–590. doi:10.1007/s00397-007-0254-z

Lin NYC, Goyal S, Cheng X, Zia RN, Escobedo FA, Cohen I (2013) Far-from-equilibrium sheared colloidal liquids: disentangling relaxation, advection, and shear-induced diffusion. Phys Rev E 88:062309. doi:10.1103/PhysRevE.88.062309

López-Barrón CR, Porcar L, Eberle APR, Wagner NJ (2012) Dynamics of melting and recrystallization in a polymeric micellar crystal subjected to large amplitude oscillatory shear flow. Phys Rev Lett 108: 258301. doi:10.1103/PhysRevLett.108.258301

Lund R, Willner L, Stellbrink J, Lindner P, Richter D (2006) Logarithmic chain-exchange kinetics of diblock copolymer micelles. Physical Review Letters 96. doi:10.1103/PhysRevLett.96.068302

Mason T, Bibette J, Weitz D (1996) Yielding and flow of monodisperse emulsions. J Colloid Interface Sci 179:439–448

Mason TG, Weitz DA (1995) Linear viscoelasticity of colloidal hard sphere suspensions near the glass transition. Phys Rev Lett 75: 2770–2773. doi:10.1103/PhysRevLett.75.2770

Merger D, Wilhelm M (2014) Intrinsic nonlinearity from LAOStrain-experiments on various strain- and stress-controlled rheometers: a quantitative comparison. Rheol Acta 53:621–634. doi:10.1007/s00397-014-0781-3

Mewis J, Wagner NJ (2011) Colloidal suspension rheology. Cambridge University Press

Nicolai T, Benyahia L (2005) Shear flow and large strain oscillation of dense polymeric micelle suspension. Macromolecules 38:9794–9802. doi:10.1021/ma0514267

Petekidis G, Vlassopoulos D, Pusey PN (2003) Yielding and flow of colloidal glasses. Faraday Discuss 123:287–302. doi:10.1039/b207343a

Pham KN, Petekidis G, Vlassopoulos D, Egelhaaf SU, Pusey PN, Poon WCK (2006) Yielding of colloidal glasses. Europhys Lett 75:624–630. doi:10.1209/epl/i2006-10156-y

Philippoff W (1966) Vibrational measurements with large amplitudes. Transactions of The Society of Rheology (1957–1977) 10:317–334

Poulos AS, Stellbrink J, Petekidis G (2013) Flow of concentrated solutions of starlike micelles under large-amplitude oscillatory shear. Rheol Acta 52:785–800. doi:10.1007/s00397-013-0703-9

Pusey PN, van Megen W (1987) Observation of a glass transition in suspensions of spherical colloidal particles. Phys Rev Lett 59: 2083–2086. doi:10.1103/PhysRevLett.59.2083

Renou F, Stellbrink J, Petekidis G (2010a) Yielding processes in a colloidal glass of soft star-like micelles under large amplitude oscillatory shear (LAOS). J Rheol 54:1219. doi:10.1122/1.3483610

Rogers SA, Erwin BM, Vlassopoulos D, Cloitre M (2011) A sequence of physical processes determined and quantified in LAOS: application to a yield stress fluid. J Rheol 55:435. doi:10.1122/1.3544591

Schlatter G, Fleury G, Muller R (2005) Fourier transform rheology of branched polyethylene: experiments and models for assessing the macromolecular architecture. Macromolecules 38:6492–6503. doi:10.1021/ma0505530

Senff H, Richtering W (1999) Temperature sensitive microgel suspensions: colloidal phase behavior and rheology of soft spheres. J Chem Phys 111:1705. doi:10.1063/1.479430

Sollich P (1998) Rheological constitutive equation for a model of soft glassy materials. Phys Rev E 58:738

Stellbrink J, Rother G, Laurati M, Lund R, Willner L, Richter D (2004) Poly(ethylene-alt-propylene)–poly(ethylene oxide) diblock copolymer micelles: a colloidal model system with tunable softness. J Phys Condens Matter 16:S3821–S3834. doi:10.1088/0953-8984/16/38/004

Stiakakis E, Vlassopoulos D, Loppinet B, Roovers J, Meier G (2002) Kinetic arrest of crowded soft spheres in solvents of varying quality. Phys Rev E 66:051804

Stiakakis E, Wilk A, Kohlbrecher J, Vlassopoulos D, Petekidis G (2010) Slow dynamics, aging, and crystallization of multiarm star glasses. Phys Rev E 81. doi:10.1103/PhysRevE.81.020402

van der Vaart K, Rahmani Y, Zargar R, Hu ZB, Bonn D, Schall P (2013) Rheology of concentrated soft and hard-sphere suspensions. J Rheol 57:1195–1209. doi:10.1122/1.4808054

Wilhelm M, Maring D, Spiess HW (1998) Fourier-transform rheology. Rheol Acta 37:399–405. doi:10.1007/s003970050126

Wilhelm M, Reinheimer P, Ortseifer M (1999) High sensitivity fourier-transform rheology. Rheol Acta 38:349–356. doi:10.1007/s003970050185

Wilhelm M, Reinheimer P, Ortseifer M, Neidhofer T, Spiess HW (2000) The crossover between linear and non-linear mechanical behaviour in polymer solutions as detected by Fourier-transform rheology. Rheol Acta 39:241–246. doi:10.1007/s003970000084